

Spatially resolved and clinically feasible relaxation-diffusion correlation spectroscopy in the spinal cord

Dan Benjamini and Peter J Basser

Section on Quantitative Imaging and Tissue Sciences, NICHD, National Institutes of Health, Bethesda, MD 20892, USA

Introduction: Combining and correlating multidimensional magnetic resonance (MR) contrast mechanisms, e.g., D - T_2 , would provide novel and complementary information about dynamic molecular processes and microscopic physical and chemical environments within tissue. To date, these multidimensional relaxation-diffusion correlation (REDCO) experiments have been primarily relegated to applications involving NMR spectrometry and spectroscopy studies in homogeneous samples [1–3]. However, these methods have not been widely used in MRI applications owing to the vast amount of scan time and acquired MR data required to reconstruct a single multidimensional spectrum. To overcome this bottleneck we recently proposed the marginal distributions constrained optimization (MADCO) method for accelerated multidimensional MRI [4]. The concept in this approach is to use the more accessible 1D information (i.e., the marginal distributions) to enforce physical constraints on the multidimensional distribution, resulting in a dramatic reduction in the number of data samples required and a concomitant reduction in MRI acquisition times [4]. Here, by using MADCO, we introduce a new MR imaging framework—which we term magnetic resonance microdynamic imaging (MRMI)—that permits the simultaneous noninvasive quantification of multiple cellular, interstitial, and subcellular tissue components within tissue. This unique information is obtained without imposing *a priori* tissue models, and in a clinically or biologically feasible time period.

Materials and Methods: Although it can be used to investigate other types of biological tissue, we chose to apply MRMI on a fixed ferret spinal cord specimen because its microstructure and organization are well known and highly ordered. MRI data were collected on a 7 T Bruker wide-bore vertical magnet with an AVANCE III MRI spectrometer equipped with a Micro2.5 microimaging probe and three GREAT60 gradient amplifiers. MRI data were acquired with an inversion recovery spin-echo diffusion-weighted echo planar imaging (IR-DWI-EPI) sequence, in which the diffusion gradient amplitude, G , the inversion period, τ_1 , and the echo time, τ_2 , governed the diffusion, T_1 , and T_2 weightings, respectively. The three 1D distributions of T_1 , T_2 , and D , were first estimated using a total of 52 acquisitions in the G - τ_1 - τ_2 space. The MADCO framework was then used with the *a priori* obtained 1D distributions as constraints to estimate the D - T_1 , D - T_2 , and T_1 - T_2 spectra, using an additional 36 acquisitions. For all types of acquisitions, TR = inversion time + 4 s. A single 2.5 mm axial slice with in-plane resolution of $101 \times 101 \mu\text{m}^2$ was acquired with 2 averages and 8 segments. Each image took 1 minute to acquire, leading to a total experimental time of 88 min.

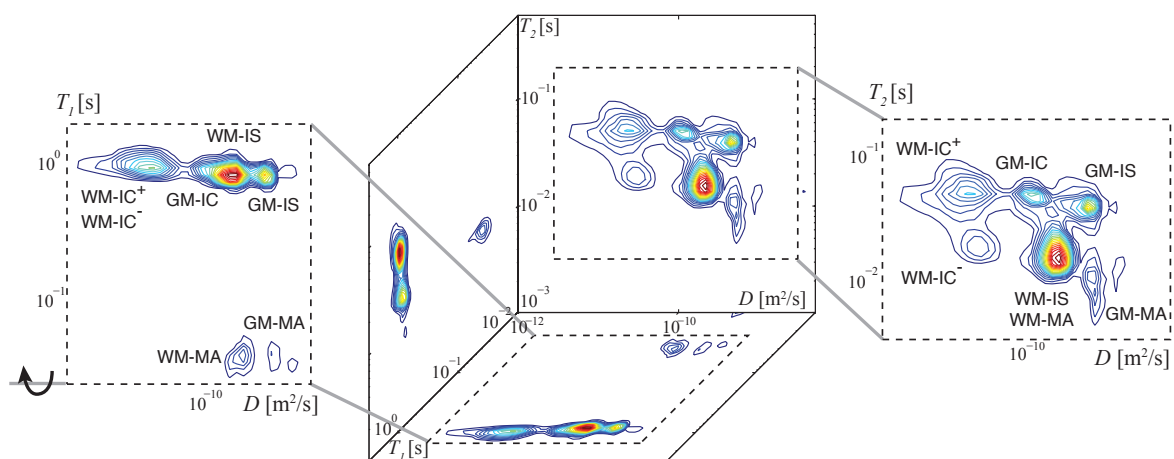


Figure 1: Microscopic compartmental analysis of a mixture of the representative gray and white matter ROIs, which yield a gray–white matter “mixed volume”. To the right is the most informative D - T_2 spectrum with four peaks, corresponding to four unique microscopic nervous components that can be unequivocally assigned (WM-IC⁺, WM-IC⁻, GM-IC, and GM-IS). Having similar T_2 and D values, the WM-IS, WM-MA, and GM-MA peaks are well separated by their T_1 value, reflected in the D - T_1 spectrum to the left.

Results and Discussion: In most cases, a typical MRI brain voxel would include gray and white matter (GM and WM), and would contain a mixture of axons, neurons, different types of glia, myelin, interstitial spaces, and proteins. One of the greatest challenges facing quantitative MRI methods is distinguishing between at least a subset of these components within an imaging voxel. The strength of microdynamic imaging in this context was demonstrated by analyzing a mixture of spectra from GM and WM regions of interest (ROIs). The resulting REDCO spectra are shown in **Fig. 1**, in which the microdynamic information from the D - T_2 and D - T_1 spectra reveals seven unique

peaks: (1) WM interstitial (WM-IS); WM intracellular (WM-IC), which has two subpopulations – with (2) long T_2 (WM-IC⁺) and (3) short T_2 (WM-IC⁻) values; a low diffusivity short-lived T_1 and T_2 peak that is assigned to (4) WM myelin-associated (WM-MA) water; (5) GM intracellular (GM-IC); (6) GM interstitial space (GM-IS); and a short T_1 - T_2 GM component is identified as a (7) GM myelin-associated (GM-MA) component. To associate the REDCO peaks to their correct *macroenvironment* (i.e., WM or GM), “pure” WM and GM ROIs were first selected and analyzed separately.

Summing over the REDCO peaks resulted in the *apparent volume fraction* (AVF) images of the nervous tissue components, which exhibit unique contrasts and are shown in **Fig. 2**. First, let us examine the spatial distribution of all the intracellular components we identified: WM-IC⁺, WM-IC⁻, and GM-IC. The difference between the intracellular images is clear, with the practical absence of WM-IC⁻ in the gray column (**Fig. 2a**). On the other hand, the GM-IC is mainly present in the GM (**Fig. 2b**). The third IC component, the WM-IC⁺ image, reveals a more uniform spatial distribution of intensities, with higher AVFs in WM (**Fig. 2c**). We note that very few axons, if any, are expected to reside in the cervical portion of the spinal cord GM, while neurons should be mostly present there and not in the WM [5]. On the other hand, glia range in size and shape (i.e., microglia and macroglia) and are distributed in all CNS tissue types, with more in WM than in other tissue types [6]. Apart from the known neuroanatomy, it is visible from **Fig. 1** that the GM-IC component has the highest diffusivity among the three cellular components, which means that GM-IC water resides in the biggest physical compartment. It is also evident that the WM-IC⁺ peak spans a wide range of diffusivities, suggesting a broad size distribution. With this in mind, and with the clear difference in the image contrasts, the WM-IC⁻, WM-IC⁺, and GM-IC components can be hypothesized to originate from intraaxonal, intragial, and intraneuronal water, respectively. As anticipated, WM-IS image intensity is mainly limited to WM (**Fig. 2d**) and is complementary to the GM-IS image, whose intensity is almost exclusively present in the gray column (**Fig. 2e**). The total myelin-associated content (WM-MA + GM-MA) MRI stain suggests a higher concentration in WM, but non negligible presence in the GM as well (**Fig. 2f**). Myelin-associated proteins, such as myelin basic protein and myelin oligodendrocyte glycoprotein, are present in both myelin and in oligodendrocytes. While myelin is almost exclusively present in WM, oligodendrocytes are present in GM as well, which is consistent with the observed MA image contrast.

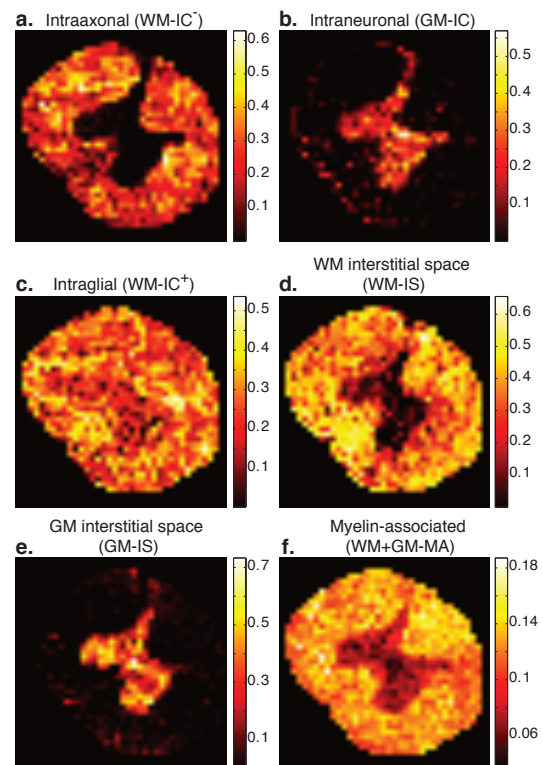


Figure 2: Generated quantitative images of the identified microscopic neuroanatomical tissue components. Note that the AVFs are additive and normalized, and therefore sum to 1.

Conclusions: Using MRMI, we identified specific tissue components on the basis of their multispectral signature within individual imaging voxels. The spatially resolved images obtained by combining REDCO and MRI allowed us, for the first time, to detect and distinguish between different intracellular components: axons, neurons, and glia. Interstitial spaces and myelin-associated water, which are additional distinct microenvironments within gray and white matter, were also identified and imaged. These seven cellular, interstitial, and extracellular components may be present in any single MRMI spinal cord voxel. MRMI delivers unprecedented microdynamic imaging data, which could have only been obtained by using laborious histological procedures on fixed specimen. MRMI is clearly not limited to applications within the CNS; it can be used on any type of tissue or material in which relaxation, diffusion, and transport properties can be measured, providing exciting opportunities for investigators in a range of disciplines.

References

- [1] A. E. English *et al.* Quantitative Two-Dimensional time Correlation Relaxometry. *Magn Reson Med*, 22(2):425–434, 1991.
- [2] Mark D. Does *et al.* Multi-component T1 relaxation and magnetisation transfer in peripheral nerve. *Magn Reson Imaging*, 16(9):1033–1041, 1998.
- [3] Yi-Qiao Song *et al.* T1-T2 Correlation Spectra Obtained Using a Fast Two-Dimensional Laplace Inversion. *J Magn Reson*, 154(2):261–268, 2002.
- [4] Dan Benjamini and Peter J. Basser. Use of marginal distributions constrained optimization (MADCO) for accelerated 2D MRI relaxometry and diffusometry. *J Magn Reson*, 271:40–45, 2016.
- [5] Susan Standring. *Gray’s Anatomy: The Anatomical Basis of Clinical Practice*. Elsevier, 41 edition, 2015.
- [6] Richard S Snell. *Clinical Neuroanatomy*. Lippincott Williams & Wilkins, Philadelphia, PA, 7th edition, 2009.